Spin filtering with EuO: Insight from the complex band structure

Pavel V. Lukashev,[1] Aleksander L. Wysocki,[1,2] Julian P. Velev,[3] Mark van Schilfgaarde,[4] Sitaram S. Jaswal,[1]
Kirill D. Belashchenko,[1] and Evgeny Y. Tsymbal[1,*]

[1]*Department of Physics and Astronomy & Nebraska Center for Materials and Nanoscience, University of Nebraska, Lincoln, Nebraska 68588, USA*

[2]*School of Applied Engineering Physics, Cornell University, Ithaca, New York 14853, USA*

[3]*Department of Physics, Institute for Functional Nanomaterials, University of Puerto Rico, San Juan, Puerto Rico 00931, USA*

[4]*Department of Physics, Kings College London, London WC2R 2LS, England, United Kingdom*

(Received 23 April 2012; published 14 June 2012)

Spin-filter tunneling is a promising way to create highly-spin-polarized currents. So far the understanding of the spin-filtering effect has been limited to a free-electron description based on the spin-dependent tunneling barrier height. In this work we explore the complex of EuO as a representative ferromagnetic insulator used in spin-filter tunneling experiments and show that the mechanism of spin filtering is more intricate than it has been previously thought. We demonstrate the importance of the multiorbital band structure with an indirect band gap for spin-filter tunneling. By analyzing the symmetry of the complex bands and the decay rates for different wave vectors and energies we draw conclusions about spin-filter efficiency of EuO. Our results provide guidelines for the design of spin-filter tunnel junctions with enhanced spin polarization.

DOI: 10.1103/PhysRevB.85.224414 PACS number(s): 72.25.−b, 71.20.Ps, 73.40.Gk, 75.47.Lx

I. INTRODUCTION

Attaining sizable spin polarization of electric current is an important constituent of spintronics—an emerging technology that exploits an electron's spin in solid-state electronic devices.[1] One of the promising approaches to realize the high spin polarization is to employ spin-filter tunneling, where spin-filter material, typically a ferromagnetic or ferrimagnetic insulator, is used as a barrier in a tunnel junction.[2] The implementation of spin-filter tunneling is considered as an alternative to a more conventional approach based on magnetic tunnel junctions. The latter consists of two ferromagnetic electrodes separated by a nonmagnetic insulating barrier and its resistance depends of relative magnetization orientation of the electrodes, the effect known as tunneling magnetoresistance (TMR).[3–5]

The basic idea behind spin-filter tunneling is to exploit the spin-dependent barrier of a ferromagnetic or ferrimagnetic insulator to achieve considerably different transmission probabilities for electrons with opposite spin directions. Due to the exchange splitting of the spin bands, the conduction-band minimum (CBM) in these materials lies at different energies for majority- and minority-spin electrons, which yields a spin-dependent tunneling barrier. Due to the exponential dependence of the tunneling transmission on the barrier height, electrons are expected to be transmitted with significantly different probabilities depending on their spin.

Early experiments on EuS (Ref. 6) and EuSe (Ref. 7) and more recently on EuO (Ref. 8) have demonstrated the potential of spin-filter tunneling using the Tedrow-Meservey technique,[9] which allows a direct measurement of tunneling spin polarization. The Curie temperature of Eu chalcogenides is relatively low, and more recent efforts have focused on searching for spin-filter materials to achieve functioning at room temperature using epitaxial tunnel junctions. In order to realize the spin-filtering effect in a tunnel junction, a ferromagnetic counter electrode is added. Depending on the relative magnetization orientation of the barrier and the counter electrode, the tunneling current is expected to be altered due to a TMR effect. Complex oxide materials such as $CoFe_2O_4$,[10,11] $NiFe_2O_4$,[12] $NiMn_2O_4$,[13] $BiMnO_3$,[14] $CoCr_2O_4$,[15] and $MnCr_2O_4$ (Ref. 15) have been studied. Unfortunately, in all cases, the observed TMR values are rather small, with the largest 25% observed at room temperature for $CoFe_2O_4$.[10]

A theoretical description of spin-filter tunneling has been limited so far to a simple approach based on a free-electron model.[2,16] Within this model an exponential decay of the wave function in the ferromagnetic tunneling barrier is determined entirely by the spin-dependent barrier height. The decay rates $\kappa_{\uparrow,\downarrow}$ of the evanescent states depend on spin through the exchange splitting Δ_{ex} of spin bands so that $\kappa_{\uparrow,\downarrow} = \sqrt{2m(U \pm \Delta_{ex}/2)}/\hbar$, where U is the tunneling barrier height in a paramagnetic state of the insulator and m is the effective mass. Within this model spin-filter efficiency is fully controlled by $\kappa_{\uparrow,\downarrow}$ and barrier thickness d through transmission probability $\sim e^{-2\kappa_{\uparrow,\downarrow}d}$.

This description ignores, however, the multiband nature of ferromagnetic insulators. In particular, it neglects the effects related to different symmetries of the bands and their orbital character. In contrast, it is known that tunneling through insulators can be understood in terms of the evanescent states[17] and the method to investigate them is the complex band structure in the energy gap region.[18–21] So far, however, this approach has not been applied to spin-filter materials such as EuO. It has recently been shown, both theoretically using reliable GW calculations[22] and experimentally using angle-resolved photoemission experiments,[23] that the band gap in EuO is indirect, with the conduction-band minimum being located at the X point in the Brillouin zone.

In this paper we employ the local-density approximation including a Hubbard U term accounting for the on-site Coulomb interaction (LDA + U) method[24] to perform a detailed analysis of the evanescent states in EuO as a representative spin-filter material. We demonstrate the significance of the multiorbital

band structure with an indirect band gap for spin-filter tunneling. By analyzing the symmetry of these complex bands and decay rates for different transverse wave vectors and energies we draw conclusions about the spin-filter efficiency of EuO.

II. METHODS

EuO is a ferromagnetic insulator with a rocksalt crystal structure and a bulk Curie temperature of 69 K. A divalent Eu ion in EuO has a half-filled $4f$ shell forming the ${}^8S_{7/2}$ ionic multiplet and a magnetization of $7\mu_B$ per Eu ion. The exchange coupling between the localized $4f$ electrons causes the ferromagnetic ordering in EuO. The half-filled $4f$ band is separated from the $5d$–$6s$ conduction bands by a band gap of about 1eV at room temperature.[25] In the ferromagnetic state of EuO the intra-atomic exchange interaction between the $4f$ and $5d$ Eu states leads to spin splitting of the conduction band $\Delta_{\rm ex} \approx 0.6$ eV.[26] This spin splitting is responsible for the spin-dependent barrier in spin-filter tunneling experiments.[8]

To elucidate the mechanism of spin filtering in EuO we perform electronic band-structure calculations using the scalar-relativistic principal-layer Green's-function version[27,28] of the tight-binding linear muffin-tin orbital (LMTO) method[29] in the atomic sphere approximation and the LDA + U approach.[24] In the calculations we use the experimental lattice constant of EuO, $a = 5.14$ Å. To achieve an accurate description of the band structure, we set $J = 0.58$ eV (Ref. 22) and adjust the value of U for the Eu $4f$ orbitals while adding energy shifts V_{6s} for the Eu $6s$ states and V_{2p} for the O $2p$ states to bring the valence and conduction bands in agreement with the GW results.[22] We find the best match between the LDA + U and GW bands for $U = 8.84$ eV, $V_{6s} = -0.61$ eV, and $V_{2p} = -0.14$ eV. The resulting band gap of 0.90 eV at the X point is consistent with the experimental value of 0.95 eV (Ref. 30) and the exchange splitting of the Eu $5d$ bands is $\Delta_{\rm ex} = 0.70$ eV.

We investigate the complex band structure of EuO using the difference-equation method.[31] The LDA + U correction for the Eu $4f$ orbitals is applied in a simplified way by shifting the majority-spin (minority-spin) $4f$ states down (up) by $(U + 6J)/2$. These shifts (along with the empirical shifts for Eu $6s$ and O $2p$ orbitals) are added to the LMTO band-center parameter C and to the linearization energy E_ν in the third-order parametrization of the potential function $P(E)$. For EuO this is an excellent approximation because the occupation numbers for majority-spin (minority-spin) $4f$ states are very close to 1 (0).

III. RESULTS

An arbitrary wave vector consists of a component parallel to the interface $\mathbf{k}_\parallel$, which is conserved during tunneling, and a component perpendicular to the interface k_z. For each $\mathbf{k}_\parallel$ we calculate the dispersion relation $E = E(k_z)$, allowing complex $k_z = q + i\kappa$. The imaginary part κ is the decay rate, so the corresponding wave functions decay as $\sim e^{-\kappa z}$. In EuO, both the real and complex bands are spin dependent.

Figure 1 shows the calculated spin-dependent complex band structure of EuO for $\mathbf{k}_\parallel = 0$ in the Δ direction, i.e., $\Gamma \to X$ (see the inset of Fig. 1). The complex bands (left and right panels)

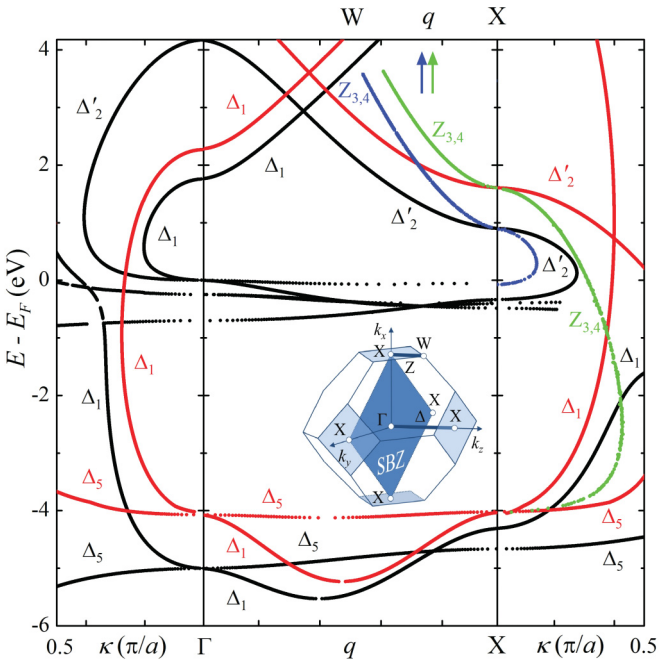

FIG. 1. (Color online) Complex band structure of EuO in the Δ direction ($\Gamma \to X$) at $q = 0$ (left panel) and $q = \pi/a$ (right panel) for majority (black dots) and minority (red dots) spin and in the Z direction ($X \to W$) at $q = 0$ (right panel) for majority (blue dots) and minority (green dots) spin. The middle panel shows real bands. The inset shows symmetry points and lines in the Brillouin zone of bulk EuO and the surface Brillouin zone.

are connected to the real bands (middle panel) at the Γ and X points and inherit their symmetry properties. The curvature at the connecting points is the same for the real and complex bands due to the analytic properties of the $E(k_z)$ function.[17]

In a tunnel junction the Fermi level lies within the insulator band gap and the evanescent state that has the lowest decay rate at this energy dominates the conductance in the thick barrier limit. The symmetry of this state as determined by its orbital character is of primary importance because it determines the Bloch states in the electrodes that can couple to it and contribute to the transmission. In ferromagnetic insulators the evanescent states are spin dependent and thus their symmetry strongly affects spin filtering.

From Fig. 1 we see that in the band gap of EuO lying in the energy interval from 0 to 0.9 eV there are two evanescent states, one in each spin channel, that have relatively small decay rates: one with Δ_2' symmetry (the respective wave function transforms as xy) and the other with Δ_1 symmetry (the identity representation). The Δ_2' evanescent state inherits its symmetry from the exchange-split Eu $4d$ state at the bottom of the conduction band (the X point). The Δ_1 evanescent state is connected to the Γ-point Eu $6s$ state that lies at about 2 eV in the conduction band.

Within the standard free-electron picture the highest spin efficiency may be obtained if the Fermi level lies very close to the CBM where the majority-spin decay rate approaches zero $\kappa_\uparrow \to 0$, whereas the minority-spin decay rate remains finite $\kappa_\downarrow \approx \sqrt{2m\Delta_{\rm ex}}/\hbar$. However, this argument assumes that the electrodes also have a Δ_2' symmetric state, which is not the case for Cu and Al and for the noble metals Ag and Au. The Δ_1

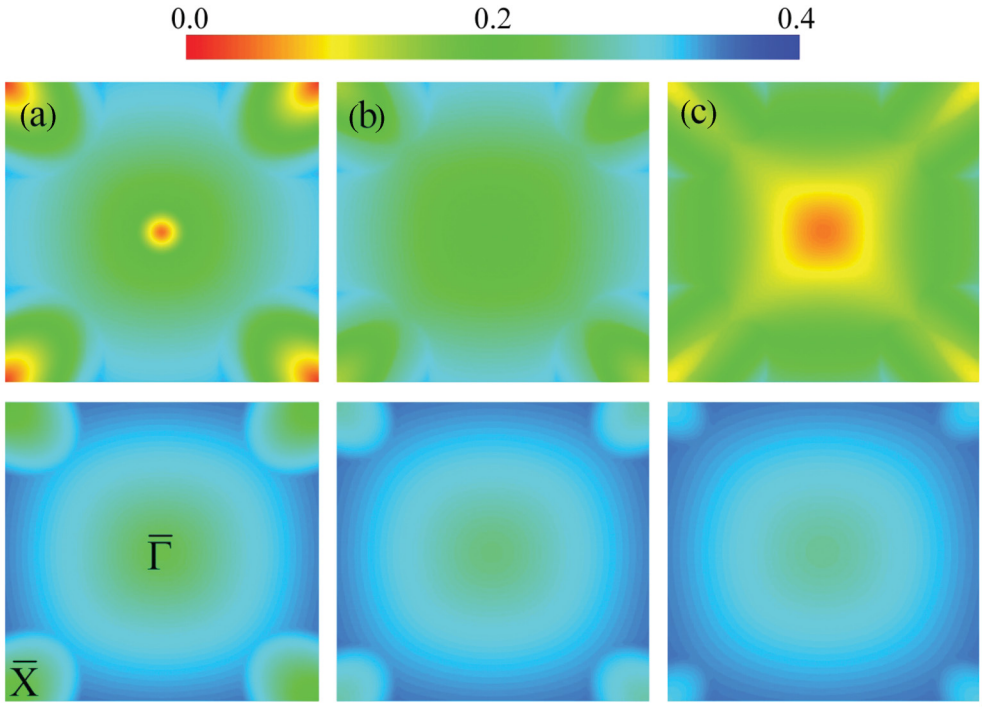

FIG. 2. (Color online) Lowest decay rate (in units of π/a) of the majority-spin (top panels) and minority-spin (bottom panels) evanescent states in the band gap of EuO as a function of $\mathbf{k}_\parallel$ in the SBZ at (a) $E = 0.89$ eV, (b) $E = 0.45$ eV, and (c) $E = 0.01$ eV.

symmetric state that is available at the Fermi energy in these free-electron-like metals would tunnel through the EuO Δ_1 evanescent state, whose much larger decay rate has a relatively small spin asymmetry in the vicinity of the conduction band. For example, at $E = 0.89$ eV (i.e., 0.01 eV below the CBM) and $\mathbf{k}_\parallel = 0$ we find $\kappa_\uparrow \approx 0.118$ Å^{-1} and $\kappa_\downarrow \approx 0.144$ Å^{-1} for this state. If this state dominates the transmission $\sim e^{-2\kappa_{\uparrow,\downarrow}d}$, we find for a typical insulator thickness $d = 2$ nm the spin polarization $P = \tanh[(\kappa_\downarrow - \kappa_\uparrow)d]$ of about 50%, which is not too impressive for a spin filter.[32] Using metals that have d bands of Δ_2' symmetry at the Fermi energy may enhance spin filtering across EuO.

Assuming the dominant contribution to conductance at the $\bar{\Gamma}$ point is, however, unjustified because the band gap in EuO is indirect. This behavior is revealed by the distribution of the decay rates as a function of $\mathbf{k}_\parallel$ in the surface Brillouin zone (SBZ) shown in Fig. 2. For $E = 0.89$ eV (in the vicinity of the CBM), we see from Fig. 2(a) that κ reaches its global minimum at the $\bar{X}$ point rather than at the $\bar{\Gamma}$ point. This feature originates from the anisotropy of the effective mass at the X point in the Brillouin zone of bulk EuO. This anisotropy is seen in Fig. 1 from the comparison of the real bands along the Δ ($\Gamma \to X$) and Z ($X \to W$) lines, which clearly have different curvatures [compare black (red) and blue (green) lines]. We find that the effective mass is $m_{\bar{\Gamma}} \approx 0.3m_e$ along the Δ line, whereas $m_{\bar{X}} \approx 0.12m_e$ along the Z line (here m_e is the free-electron mass). Due to the complex bands near the X point forming an analytic continuation of the real bands, the anisotropic curvature is inherited by the evanescent states in the band gap. Since the Δ line in the bulk Brillouin zone is projected to the $\bar{\Gamma}$ point and the Z line to the $\bar{X}$ point in the SBZ, the decay rate at $\bar{X}$ is lower than that at $\bar{\Gamma}$ [see Fig. 2(a) and also Fig. 1]. The decay rates for energies E close to the CBM (E_{CBM}) are given by $\kappa_{\bar{\Gamma},\bar{X}} = \sqrt{2m_{\bar{\Gamma},\bar{X}}(E_{\mathrm{CBM}} - E)}/\hbar$.

There is a sizable difference in the decay rates for majority- and minority-spin electrons at the $\bar{X}$ point [compare the top and bottom panels in Fig. 2(a)]. To achieve spin filtering through this channel the electrodes should supply Bloch states of the Z_3 (Z_4) symmetry representation, which involves a linear combination of functions with x and xz (y and yz) symmetries in the Z direction. These states originate from the p and d orbitals and thus metals with these orbitals at the Fermi energy are required as electrodes.

For energies close to the middle of the band gap, e.g., $E = 0.45$ eV, the spin asymmetry in the decay rates is reduced. At the $\bar{\Gamma}$ point the Δ_1 state has the lowest decay rate for both majority- and minority-spin electrons (see Fig. 1). In this case we find $\kappa_\uparrow \approx 0.122$ Å^{-1} and $\kappa_\downarrow \approx 0.156$ Å^{-1}, i.e., the spin asymmetry in κ is again relatively small. The decay rates for both spins have a global minimum at the $\bar{X}$ point [Fig. 2(b)], which has the same origin as above.

At lower energies close to the $4f$ majority-spin band the spin asymmetry may be significantly enhanced because the majority-spin Δ_1 evanescent state is connected to the $4f$ state just at the valence-band maximum (VBM), whereas the minority-spin Δ_1 complex band extends down to the O $2p$ band of the same symmetry. At the same time the majority-spin Δ_2' complex band is connected to the real $4f$ band at the X point at about 0.34 eV below the VBM, which implies that at energies close to the VBM tunneling through the Δ_1 band should dominate. This behavior is evident from Fig. 2(c), where we see a clear minimum at the $\bar{\Gamma}$ point in the majority-spin channel and a large asymmetry between the majority- and minority-spin decay rates. We note, however, that in order to

achieve significant spin selectivity the Fermi energy needs to lie very close to the VBM because the f states are heavy and moving up into the gap from the edge of the valence band leads to a significant increase in κ.

Finally, we note that interface states may add additional features in spin-filtering process that are not discussed in this paper. It is known that interfaces may sustain resonant states that can contribute to the conductance through hybridization with the electrode bulk states (see Refs. 33 and 34 for recent reviews). If the spin-filter thickness is sufficiently small, resonant tunneling may contribute to the conductance in a way not described based on bulk properties of the insulator and the electrodes separately.[35] In order to take the contribution from the interface states into account, a detailed analysis of the electronic and transport properties of the whole tunnel junction is needed. A separate consideration is also required for including effects of spin-orbit interaction[36] and defects, such as oxygen vacancies.[37]

IV. CONCLUSION

In conclusion, we have shown that under certain conditions EuO may be used as an efficient spin filter in spin-dependent tunneling experiments. However, the mechanism of spin filtering deviates significantly from the standard free-electron picture and involves effects associated with the symmetry of spin-dependent evanescent states and the dependence of the decay constant on the transverse wave vector. We find that free-electron-like bands of the Δ_1 symmetry may provide significant tunneling spin selectivity if the Fermi energy lies very close to the top of the EuO valence band. For the Fermi energy in the middle of the band gap the spin selectivity is relatively small. When the Fermi energy lies close to the CBM the large spin selectivity may be achieved if the electrodes have Δ_2' and/or Z_3 (Z_4) bands in their real band structure. These results provide an insight into the understanding of spin-filter tunneling and may help design spin-filter devices with enhanced spin polarization.

ACKNOWLEDGMENTS

This research was supported by the National Science Foundation (NSF) through the Nebraska Materials Research Science and Engineering Center (Grant No. DMR-0820521) and the Nebraska Experimental Program to Stimulate Competitive Research (Grant No. EPS-1010674). The work at the University of Puerto Rico was supported by NSF Grants No. DMR-1105474 and No. EPS-1010094. K.D.B. is supported by the Research Corporation through a Cottrell Scholar Award and by the NSF (Grant No. DMR-1005642). P.V.L. thanks Tula Paudel for helpful discussions. Computations were performed at the University of Nebraska Holland Computing Center.

*tsymbal@unl.edu

[1] I. Žutić, J. Fabian, and S. Das Sarma, Rev. Mod. Phys. **76**, 323 (2004).
[2] T. S. Santos and J. S. Moodera, in *Handbook of Spin Transport and Magnetism*, edited by E. Y. Tsymbal and I. Žutić (CRC, Boca Raton, FL, 2011), Chap. 13, p. 251.
[3] E. Y. Tsymbal, O. N. Mryasov, and P. R. LeClair, J. Phys.: Condens. Matter **15**, R109 (2003).
[4] S. Yuasa, in *Handbook of Spin Transport and Magnetism*, edited by E. Y. Tsymbal and I. Žutić (CRC, Boca Raton, FL, 2011), Chap. 11, p. 217.
[5] K. D. Belashchenko and E. Y. Tsymbal, in *Handbook of Spin Transport and Magnetism*, edited by E. Y. Tsymbal and I. Žutić (CRC, Boca Raton, FL, 2011), Chap. 12, p. 233.
[6] J. S. Moodera, X. Hao, G. A. Gibson, and R. Meservey, Phys. Rev. Lett. **61**, 637 (1988).
[7] J. S. Moodera, R. Meservey, and X. Hao, Phys. Rev. Lett. **70**, 853 (1993).
[8] T. Santos and J. Moodera, Phys. Rev. B **69**, 241203(R) (2004).
[9] R. Meservey and P. M. Tedrow, Phys. Rep. **238**, 173 (1994).
[10] M. G. Chapline and S. X. Wang, Phys. Rev. B **74**, 014418 (2006).
[11] A. V. Ramos, M. J. Guittet, J. B. Moussy, R. Mattana, C. Deranlot, F. Petroff, and C. Gatel, Appl. Phys. Lett. **91**, 122107 (2007).
[12] U. Lüders, M. Bibes, K. Bouzehouane, E. Jacquet, J.-P. Contour, S. Fusil, J.-F. Bobo, J. Fontcuberta, A. Barthélémy, and A. Fert, Appl. Phys. Lett. **88**, 082505 (2006).
[13] B. B. Nelson-Cheeseman, R. V. Chopdekar, L. M. B. Alldredge, J. S. Bettinger, E. Arenholz, and Y. Suzuki, Phys. Rev. B **76**, 220410(R) (2007).
[14] M. Gajek, M. Bibes, A. Barthélémy, K. Bouzehouane, S. Fusil, M. Varela, J. Fontcuberta, and A. Fert, Phys. Rev. B **72**, 020406(R) (2005).
[15] R. V. Chopdekar, B. B. Nelson-Cheeseman, M. Liberati, E. Arenholz, and Y. Suzuki, Phys. Rev. B **83**, 224426 (2011).
[16] M. Müller, G.-X. Miao, and J. S. Moodera, Europhys. Lett. **88**, 47006 (2009); Phys. Rev. Lett. **102**, 076601 (2009).
[17] V. Heine, Proc. Phys. Soc. London **81**, 300 (1962); Phys. Rev. **138**, A1689 (1965).
[18] P. Mavropoulos, N. Papanikolaou, and P. Dederichs, Phys. Rev. Lett. **85**, 1088 (2000).
[19] W. H. Butler, X.-G. Zhang, T. C. Schulthess, and J. M. MacLaren, Phys. Rev. B **63**, 054416 (2001).
[20] J. P. Velev, K. D. Belashchenko, D. Stewart, M. van Schilfgaarde, S. S. Jaswal, and E. Y. Tsymbal, Phys. Rev. Lett. **95**, 216601 (2005).
[21] D. Wortmann and S. Blügel, Phys. Rev. B **83**, 155114 (2011).
[22] J. An, S. Barabash, V. Ozolins, M. van Schilfgaarde, and K. Belashchenko, Phys. Rev. B **83**, 064105 (2011).
[23] J. A. Colon-Santana, J. M. An, N. Wu, K. D. Belashchenko, X. Wang, P. Liu, J. Tang, Y. Losovyj, I. N. Yakovkin, and P. A. Dowben, Phys. Rev. B **85**, 014406 (2012).
[24] A. I. Liechtenstein, V. I. Anisimov, and J. Zaanen, Phys. Rev. B **52**, R5467 (1995).
[25] A. Mauger and C. Godart, Phys. Rep. **141**, 51 (1986).
[26] P. G. Steeneken, L. H. Tjeng, I. Elfimov, G. A. Sawatzky, G. Ghiringhelli, N. B. Brookes, and D.-J. Huang, Phys. Rev. Lett. **88**, 047201 (2002).

[27]J. Kudrnovský, V. Drchal, C. Blaas, P. Weinberger, I. Turek, and P. Bruno, Phys. Rev. B **62**, 15084 (2000).
[28]S. Faleev, F. Léonard, D. Stewart, and M. van Schilfgaarde, Phys. Rev. B **71**, 195422 (2005).
[29]O. K. Andersen, Phys. Rev. B **12**, 3060 (1975).
[30]G. Busch and P. Wachter, Phys. Kondens. Mater. **5**, 232 (1966); Z. Angew. Phys. **26**, 2 (1968).
[31]A.-B. Chen, Y.-M. Lai-Hsu, and W. Chen, Phys. Rev. B **39**, 923 (1989).
[32]In fact, the spin polarization is expected to be even smaller due to the contribution to the conductance from evanescent states with $\kappa_{\parallel} \neq 0$, which have lower spin asymmetry in κ.
[33]E. Y. Tsymbal, K. D. Belashchenko, J. Velev, S. S. Jaswal, M. van Schilfgaarde, I. I. Oleynik, and D. A. Stewart, Prog. Mater. Sci. **52**, 401 (2007).
[34]J. P. Velev, P. A. Dowben, E. Y. Tsymbal, S. J. Jenkins, and A. N. Caruso, Surf. Sci. Rep. **63**, 400 (2008).
[35]K. D. Belashchenko, J. Velev, and E. Y. Tsymbal, Phys. Rev. B **72**, 140404(R) (2005).
[36]A. N. Chantis, K. D. Belashchenko, E. Y. Tsymbal, and M. van Schilfgaarde, Phys. Rev. Lett. **98**, 046601 (2007).
[37]J. Velev, K. D. Belashchenko, S. S. Jaswal, and E. Y. Tsymbal, Appl. Phys. Lett. **90**, 072502 (2007).